

# Journal of Visualized Experiments

## Injection of porcine adipose tissue-derived stroma cells via waterjet technology --Manuscript Draft--

<b>Article Type:</b>	Invited Methods Article - JoVE Produced Video
<b>Manuscript Number:</b>	JoVE63132R1
<b>Full Title:</b>	Injection of porcine adipose tissue-derived stroma cells via waterjet technology
<b>Corresponding Author:</b>	Marina Danalache Laboratory of Cell Biology Tübingen, GERMANY
<b>Corresponding Author's Institution:</b>	Laboratory of Cell Biology
<b>Corresponding Author E-Mail:</b>	danalachemarina@yahoo.com
<b>Order of Authors:</b>	Marina Danalache Jasmin Knoll Walter Linzenbold Markus Enderle Tanja Abruzzese Arnulf Stenzl Wilhelm K. Aicher
<b>Additional Information:</b>	
<b>Question</b>	<b>Response</b>
Please specify the section of the submitted manuscript.	Bioengineering
Please indicate whether this article will be Standard Access or Open Access.	Standard Access (\$1400)
Please indicate the <b>city, state/province, and country</b> where this article will be <b>filmed</b> . Please do not use abbreviations.	Tuebingen, Germany
Please confirm that you have read and agree to the terms and conditions of the author license agreement that applies below:	I agree to the <a href="#">Author License Agreement</a>
Please confirm that you have read and agree to the terms and conditions of the video release that applies below:	I agree to the <a href="#">Video Release</a>
Please provide any comments to the journal here.	

**TITLE:****Injection of Porcine Adipose Tissue-Derived Stroma Cells via Waterjet Technology****AUTHORS AND AFFILIATIONS:**

Jasmin Knoll<sup>1\*</sup>, Marina Danalache<sup>2\*</sup>, Walter Linzenbold<sup>3</sup>, Markus Enderle<sup>3</sup>, Tanja Abruzzese<sup>1</sup>, Arnulf Stenzl<sup>1</sup>, Wilhelm K. Aicher<sup>1#</sup>

<sup>1</sup> Department of Urology, University Hospital Tübingen, Tübingen, Germany

<sup>2</sup> Department of Orthopaedic Surgery, University Hospital Tübingen, Tübingen Germany

<sup>3</sup> ERBE Elektromedizin GmbH Tübingen, Germany

\*Both authors contributed equally

**# Corresponding Author:**

Prof. Dr. Wilhelm K. Aicher (aicher@uni-tuebingen.de)

**Email Addresses of Co-Authors:**

Jasmin Knoll (jasmin.knoll@med.uni-tuebingen.de)

Marina Danalache (marina.danalache@med.uni-tuebingen.de)

Walter Linzenbold (Walter.Linzenbold@erbe-med.com)

Markus Enderle (Markus.Enderle@erbe-med.com)

Tanja Abruzzese (Tanja.Abruzzese@med.uni-tuebingen.de)

Arnulf Stenzl (Urologie@med.uni-tuebingen.de)

Wilhelm K. Aicher (aicher@uni-tuebingen.de)

**KEYWORDS:**

atomic force microscopy, elasticity stromal cells, regeneration, viability, urinary incontinence, waterjet

**SUMMARY:**

We present a method of cell injection via needle free waterjet technology coupled with a sequela of post-delivery investigations in terms of cellular viability, proliferation, and elasticity measurements.

**ABSTRACT:**

Urinary incontinence (UI) is a highly prevalent condition characterized by the deficiency of the urethral sphincter muscle. Regenerative medicine branches, particularly cell therapy, are novel approaches to improve and restore the urethral sphincter function. Even though injection of active functional cells is routinely performed in clinical settings by needle and syringe, these approaches have significant disadvantages and limitations. In this context, needle-free waterjet (WJ) technology is a feasible and innovative method that can inject viable cells by visual guided cystoscopy in the urethral sphincter. In the present study, we used WJ to deliver porcine adipose tissue-derived stromal cells (pADSCs) into cadaveric urethral tissue and subsequently investigated the effect of WJ delivery on cell yield and viability. We also assessed the

biomechanical features (i.e., elasticity) by atomic force microscopy (AFM) measurements. We showed that WJ delivered pADSCs were significantly reduced in their cellular elasticity. The viability was significantly lower compared to controls but is still above 80%.

## **INTRODUCTION:**

Urinary incontinence (UI) is a widespread disorder with a prevalence of 1.8 - 30.5% in European populations<sup>1</sup> and is characterized primarily by malfunctioning of the urethral sphincter. From a clinical perspective, surgical treatment is often offered to patients when conservative therapies or physiotherapy fail to address and alleviate the emerging symptoms.

Cell therapy for the potential regenerative repair of the sphincter complex malfunction has been emerging as an avant-garde approach for the treatment of UI pathology<sup>2,3</sup>. Its main goals are to replace, repair and restore the biological functionality of the damaged tissue. In animal models for UI, stem cell transplantation has shown promising results in urodynamic outcomes<sup>2,4,5</sup>. Stem cells arise as optimal cellular candidates as they have the ability to undergo self-renewal and multipotent differentiation, thus, aiding the affected tissue regeneration<sup>6</sup>. Despite the forthcoming regenerative potential, the practical use of cell therapy remains hindered as minimally invasive delivery of cells still face several challenges concerning the injection precision and coverage of the target. Even though the current approach used for cell delivery is injection through a needle-syringe system<sup>7</sup>, it usually results in an overall deficit of viable cells, with reported viabilities as low as 1%- 31% post-transplantation<sup>8</sup>. In addition, cell delivery via needle injection has been also shown to affect the placement, the retention rate, as well as distribution of transplanted cells into the targeted tissue<sup>9-11</sup>. A feasible, novel approach that overcomes the abovementioned limitation is the needle-free cell delivery via water-jet technology.

Waterjet (WJ) technology is emerging as a new approach that enables high throughput delivery of cells by cystoscope under visual control in the urethral sphincter<sup>12,13</sup>. The WJ enables cell delivery at different pressures (E = effects in bar) ranging from E5 to E80<sup>13</sup>. In the first phase, (tissue penetration phase) isotonic solution is applied with high pressure (i.e., E60 or E80) in order to loosen the extracellular matrix surrounding the tissue targeted and open small interconnecting micro-lacunae. In the second phase (the injection phase), pressure is lowered within milliseconds (i.e., up to E10) in order to gently deliver the cells into the targeted tissue. Following this two step-phase application, the cells are not subjected to additional pressure against the tissue when ejected but are floating in a low-pressure stream into a liquid-filled cavernous area<sup>13</sup>. In an *ex vivo* model setting where stem cells were injected via WJ into cadaveric urethra tissue, viable cells could be afterwards aspirated and retrieved from the tissue and further expanded *in vitro*<sup>13</sup>. Though a 2020 study by Weber et al. demonstrated the feasibility and applicability of WJ to deliver footprint-free cardiomyocytes into the myocardium<sup>14</sup>, it has to be borne in mind the WJ technology is still in a prototype stage.

The following protocol describes how to prepare and label porcine adipose tissue-derived stromal cells (pADSC) and how to deliver them into capture fluid and cadaveric tissue via WJ technology and Williams cystoscopy needles (WN). Post cellular injection, the cellular vitality and elasticity via atomic force microscopy (AFM) is assessed. Via step-by-step instructions, the

protocol gives a clear and concise approach to acquire reliable data. The discussion section presents and describes the major advantages, limitations and future perspectives of the technique. The WJ delivery of cells as well as the sequela post translation analyses reported here are replacing the standard needle injection and provide a solid cell delivery framework for regenerative healing of the target tissue. In our recent studies we provided evidence that WJ delivered cells more precisely and at least at comparable viability when compared to needle injections<sup>15,16</sup>.

## **PROTOCOL:**

The porcine adipose tissue samples were obtained from the Institute for Experimental Surgery at the University of Tuebingen. All procedures were approved by local animal welfare authorities under the animal experiment number CU1/16.

### **1. Isolation of porcine adipose tissue-derived stromal cells**

1.1. Use porcine adipose tissue delivered from the Institute for Experimental Surgery in a 50 mL centrifuge tube to the laboratory.

1.2. Transfer the tissue to a sterile Petri dish under the sterile bench and mince it with two scalpels (No. 10) to small fragments and mush.

NOTE: Scissors can also be used in order to get small fragments. The smaller the fragments are, the better for the following digestion.

1.2.1. Transfer the small fragments/mush into a 50 mL centrifuge tube and incubate it with 5 mL of homogenizer solution for 30 min at 37 °C on a shaker. The homogenizer solution is PBS with 1% bovine serum albumin (BSA) (stock solution: 1 % (w/v) BSA in PBS) and 0.1% collagenase type I.

NOTE: Always prepare homogenizer solution freshly. The shaker has a circular shaking motion at a slow speed 25-500 rpm.

1.3. To stop the incubation, add 10 mL of growth media [Dulbecco's Modified Eagle's Medium - low glucose (DMEM-LG), 2.5% HEPES sodium salt solution (1 M), 10% fetal bovine serum (FBS), 1% L-Glutamin (200 mM), 1% Penicillin-Streptomycin (10000 U/mL Penicillin; 10,000 µg/mL Streptomycin) and 1% Amphotericin B (250 µg/mL)].

NOTE: Growth media can be prepared beforehand. Antibiotics and antifungal drugs are necessary in the preparation of the growth media for cell culture to protect cells from contaminations.

1.4. Incubate the centrifuge tubes for 10 min at room temperature.

1.5. Aspirate the fraction with adipocytes, which is lighter and therefore swimming on top of

the liquid, with a 10 mL pipette and discard it.

1.6. Filter the remaining stromal fraction through a 100  $\mu\text{m}$  cell sieve with a polyethylene terephthalate (PET) membrane free of heavy metals to withhold adipose tissue fragments and to retrieve only the cell suspension.

1.7. Centrifuge the filtered cell suspension for 7 min at 630 x g at room temperature.

1.8. Resuspend the cell pellet in 2 mL of PBS to wash the cells once.

1.9. Centrifuge the cell suspension again for 7 min at 630 x g at room temperature.

1.10. After centrifugation and repeated resuspension of the cell pellet in 10 mL of growth media per flask, seed cells in 75  $\text{cm}^2$  cell culture flasks.

NOTE: Depending on the size of the cell pellet after the washing step with PBS, seed cells in one to four flasks.

## **2. Cell cultivation of porcine adipose tissue-derived stromal cells**

2.1. Harvest and passage cells when they reach 70% confluence.

2.2. Wash cells with 10 mL of PBS twice and aspirate PBS completely.

NOTE: This step is necessary to remove remaining growth media, which is complemented by 10% FBS. FBS has several protease inhibitors which can hinder the function of the following trypsinization.

2.3. Add 3 mL of 0.05%-Trypsin-EDTA per flask to detach the cells.

2.4. Incubate flasks for 3 min at 37 °C.

2.5. Check under the microscope if cells are detached.

NOTE: Sometimes it takes some more time to detach the cells. In this case, incubate flasks for maximum 5 min at 37 °C.

2.6. To stop the incubation and detaching process, add 3 mL of growth media.

NOTE: As noted above, growth media is complemented by 10% FBS that contains protease inhibitors.

2.7. Transfer the detached cells to a centrifugation tube and centrifuge for 7 min at 630 x g at room temperature.

2.8. Resuspend the cells in 10 mL of growth media and count them with a hemocytometer.

2.9. Seed cells with an inoculation density of  $3 \times 10^5$  cells per 75 cm<sup>2</sup> flask.

### 3. Labelling of cells with calcein-AM

NOTE: Cells that are injected into cadaveric tissues are stained with a green-fluorescent membrane-permeable live-cell stain and a red-fluorescent membrane-impermeant viability indicator to verify that extracted cells are the same as the injected cells and not tissue fragments of the urethra.

3.1. Wash cells twice with 10 mL of PBS.

3.2. Add 5 mL of dye solution per 75 cm<sup>2</sup> flask. The dye solution consists of growth media with 2 µM of the green-fluorescent membrane-permeable live-cell dye and 4 µM red-fluorescent membrane-impermeant viability indicator.

3.3. Incubate for 30 min at room temperature in the dark.

3.4. Aspirate and discard the dye solution.

3.5. Wash cells again twice with 10 mL of PBS.

3.6. Add growth media and document the green and red fluorescence signal by fluorescence microscopy.

3.6.1. Place the 75 cm<sup>2</sup> flask on the microscope table, use the 10x objective, select no fluorescence filter and make sure that the transmitted light path is active.

NOTE: These steps are all performed manually on the microscope.

3.6.2. In parallel to step 3.6.1, open the software program.

3.6.3. Press the **Live** button under the **Locate** tab to obtain a live image of the cells in the flask on the table and focus on them with the coarse and fine adjustment drives.

NOTE: On the right sight the live image will appear once the **Live** button is activated.

3.6.4. In the sub-tab **Microscope Components**, select the correct objective (10x).

3.6.5. In the sub-tab **Camera**, apply a checkmark for **Auto Exposure**.

3.6.6. Press the button **Snap** to take the first picture with transmitted light.

3.6.7. Insert the scale bar by using the **Graphics** tab in the menu bar and selecting **Scale Bar**.

3.6.8. Save the image by using the **Files** tab in the menu bar and selecting **Save as czi**.

3.6.9. For the fluorescence pictures change the filter to the one specific for green or red fluorescence and select the reflected light path.

NOTE: These changes have to be done manually on the microscope.

3.6.10. Press again the **Live** button under the **Locate** tab to obtain a live image of the cells.

3.6.11. Press the button **Snap** to take the second picture with either green or red fluorescence.

3.6.12. Insert the scale bar by using the **Graphics** tab in the menu bar and selecting **Scale Bar**.

3.6.13. Save the image by using the **Files** tab in the menu bar and selecting **Save as czi**.

3.6.14. Repeat steps 3.6.9 to 3.6.13 with the other fluorescence channel.

#### **4. Prepare urethral tissue samples for injections**

4.1. Dissect the urethra and the connecting bladder out of the pig.

NOTE: Urethral tissue samples from fresh cadaveric samples of adult female landrace pigs were used for the experiments.

4.2. Transport it to the laboratory in bags on wet ice.

NOTE: The samples should be left on ice until further processing. No additives were added to the samples.

4.3. Place the urethra with the bladder on a sponge, which mimics the elasticity of the lower pelvic floor.

4.3.1. Use the bladder to determine the orientation (proximal, distal, dorsal, and ventral) of the urethra. This is possible due to the localization of the ureters and the three ligaments which fix the bladder in the abdominal and pelvic cavity. The three ligaments are the two vesicae lateralia ligaments on the sides of the bladder and the vesicae medianum, which arises from the ventral surface of the bladder (**Figure 1**).

4.4. Cut open the urethra longitudinally on the dorsal side with aid of a catheter.

4.5. Inject the cells into the opened urethra as described in the following chapters.

## 5. Injections of cells via a Williams needle in fluids and tissue samples

5.1. Harvest cells as described in step 2.

5.2. In contrast to step 2.9, adjust cell density for injections to  $2.4 \times 10^6$  cells per mL.

NOTE: For injections into tissue samples label the cells with a green-fluorescent membrane-permeable live-cell.

5.3. Aspirate the cell suspension with a syringe and apply the Williams cystoscopic injection needle (WN) to it.

5.4. Either hold the needle shortly above the 2 mL of growth media in a 15 mL centrifugation tube or insert the needle into the opened urethra tissue. In both cases inject 250  $\mu$ L of cells manually.

NOTE: Cells injected into the cadaveric urethra form an injection dome.

5.5. Collect cells injected into media directly by centrifugation for 7 min at 630 x g at room temperature.

5.6. For cells injected into the cadaveric urethra, aspirate them out of the injection dome with an 18G needle applied on a syringe.

5.7. Transfer the injected and aspirated cells into a centrifugation tube and centrifuge for 7 min at 630 x g at room temperature comparably to the cells injected into media.

5.8. After centrifugation, resuspend the cells in 4 mL of growth media in both cases.

5.9. Determine cell yield and viability by aid of Trypan blue dye exclusion with a hemocytometer.

5.9.1. Mix 20  $\mu$ L of cell suspension thoroughly with 20  $\mu$ L of Trypan blue.

5.9.2. Fill 10  $\mu$ L of this mixture in each chamber of the hemocytometer.

NOTE: Both chambers are filled and counted to gain statistical optimization by doubling sampling.

5.9.3. Under a microscope, count cells in all four corner squares.

NOTE: Count cells shining in white (unstained) as viable cells whereas cells shining blue (stained) are counted as dead cells.

5.9.4. To calculate the cell number per mL, calculate the mean of the two chambers, divide this number by two and multiply it with  $10^4$ .

## **6. Injections of cells via Waterjet in fluids and tissue samples**

6.1. Harvest cells as described in step 2.

6.2. In contrast to steps 2.9 and 5.2, adjust cell density for injections to  $6 \times 10^6$  cells per mL.

NOTE: For injections into tissue samples use cells labelled with a green-fluorescent membrane-permeable live-cell.

6.3. Fill the cell suspension into the dosing unit of the WJ device.

6.4. Either hold the injection nozzle shortly above the 2 mL of growth media in a 15 mL centrifugation tube or shortly above the opened urethra tissue.

6.5. In both cases inject 100  $\mu$ L of cells by the device using a high pressure for tissue penetration followed by a low-pressure phase for cell injections. Use the pressure settings E60-10.

NOTE: Cells injected into the cadaveric urethra form an injection dome.

6.6. Collect cells injected into media directly by centrifugation for 7 min at 630 x g at room temperature.

6.7. For cells injected into the cadaveric urethra, aspirate them out of the injection dome with an 18G needle applied on a syringe.

6.8. Transfer the injected and aspirated cells into a centrifugation tube and centrifuge for 7 min at 630 x g at room temperature comparably to the cells injected into media.

6.9. After centrifugation, resuspend cells in 4 mL of growth media in both cases.

6.10. Determine cell yield and viability by aid of Trypan blue dye exclusion with a hemocytometer as described in detail in 5.10.

## **7. Biomechanical assessment of cellular elasticity by atomic force microscopy (AFM)**

7.1. Preparation of samples

NOTE: The retrieved cells following injection are now subject for further analyses by AFM. Additionally, cells that were not injected are used as controls.

7.1.1. Seed cells in tissue culture dishes with a density of  $5 \times 10^5$  cells per dish.

NOTE: Seed one tissue culture dish per condition. The conditions are controls, ADSCs injected by WJ or WN into media and ADSCs injected by WJ or WN into cadaveric tissue.

7.1.2. Incubate cells in tissue culture dishes for 3 h at 37 °C.

NOTE: To avoid variances due to cells in G1 phase and during mitosis, we performed AFM measurements 3 h after the cell seeding step.

7.1.3. Right before the measurement with the AFM replace the growth media with 3 mL of Leibovitz's L-15 media without L-glutamine.

7.1.4. Place the tissue culture dish in the sample holder of the AFM device and turn on the Petri dish heater set at 37 °C.

7.2. Preparation of AFM and cantilever calibration

7.2.1. Use a glass block that is specified for measurements in liquids and adjust it on the AFM holder.

NOTE: The upper surface of the glass block must be straight and in parallel to the AFM holder.

7.2.2. Carefully place the cantilever on the surface of the glass block. The tip A must lay over the polished optical plane.

NOTE: Do not scratch the polished optical surface of the glass block because scratches could lead to interferences in the measurements. The tip A must protrude over the polished optical plane because otherwise the reflection of the laser of the AFM to the photodetector is not possible.

7.2.3. To stabilize the cantilever on the glass block, add a metallic spring with the aid of tweezers.

7.2.4. When the cantilever is fixed on the glass block place the block on the AFM head and lock the integrated locking mechanism.

7.2.5. Mount the AFM head on the AFM device.

NOTE: The spring must face the left side to be placed correctly. If this is not the case, correct the position of the glass block and adjust the AFM head again.

7.2.6. Initialize the software setup and open the software together with the laser alignment window and the approach parameter settings. Additionally, turn on the stepper motor, the laser light and the CCD-camera.

7.2.7. Identify the cantilever tip A by using the CCD-camera.

7.2.8. Lower the cantilever until it is fully dipped into the medium. Use the stepper motor function to reach this aim.

7.2.9. Once the cantilever is fully covered by medium, the laser is aligned on top of the cantilever by using the adjustment screws. The reflected beam must fall onto the center of the photodetector and the sum of the signals must be 1 V or higher. The lateral and vertical deflections should be close to 0.

NOTE: If the center is reached can be monitored in the laser alignment function as well as the signal values. If the signal values are not correct, further adjustments are necessary.

7.2.10. Run now the scanner **Approach** with the approach parameters (**Table 1**).

7.2.11. Retract the cantilever by 100  $\mu\text{m}$  once it reaches the bottom by pressing the **Retract** button .

NOTE: Make sure that no cell is attached at that field were the approach is done because this would falsify the calibration.

7.2.12. Set up the **Run** parameters according to the following specifications: Setpoint 1 V, Pulling Length 90  $\mu\text{m}$ , Velocity: 5  $\mu\text{m/s}$ , Sample rate: 2000 Hz and as a Delay Mode: Constant Force.

7.2.13. Start the calibration force-distance curve measuring by pressing the button **Run**.

NOTE: By clicking the **Run** button in the software a force-distance curve is obtained.

7.2.14. Select the region of linear fit of the retracted curve in the software on the obtained calibration force-distance curve. Calculate the spring constant measurement by the software.

7.2.15. Calibrate the cantilever following the exact parameters and steps as described by Danalache et al.<sup>17</sup>.

### 7.3. Measuring the elasticity of individual cells

7.3.1. Visually identify a cell and focus on it. Place the computer mouse at the middle of the cell. To improve the measurements precision, position the AFM tip directly above the cell nucleus.

NOTE: The computer mouse is used as visual marker to identify the target site of indentation.

7.3.2. Now focus on the cantilever and move it on the computer mouse.

7.3.3. Start the measurement with **Run** with the parameters given in **Table 2**.

NOTE: The set point parameter obtained by calibration of the cantilever are used. Furthermore, one cell is measured three times. Measure at least 50 cells.

#### 7.4. Data processing

7.4.1. Process the data following exact steps and parameters as previously described by Danalache<sup>17</sup>.

7.4.2. Save and export the file.

### 8. Statistical analysis

8.1. Open the statistical software.

8.2. Choose the selection of **New Dataset**.

NOTE: Two files are opened. One is the “DataSet” and the other one is the “Output” file.

8.3. Select the **DataSet** file and open the **Variable View** tab.

8.4. Insert the numeric variables for site injection (capture fluid or cadaveric tissue), category (control, WJ injection, WN injection) and elasticity.

8.5. Insert the measured elasticity data with their corresponding site injection and category number in the **Data View** tab.

8.6. Analyze the data by selecting the menu bar tab **Analyze | Descriptive Statistics** and choose **Exploratory data analysis**.

8.7. As the dependent variable, select **Elasticity** and factor list select **Category**.

NOTE: The results are displayed in the “Output” file including a box plot which is used for the results section.

8.8. To perform a statistical test, select the **Independent Samples** within the **Nonparametric Test** under the menu bar tab **Analyze**.

8.9. In the new opened file keep the settings in the tab **Objective** and **Settings**.

8.10. Open the tab **Fields** and choose **Elasticity** as Test Fields and **Category** as Groups.

8.11. Press **Run**.

NOTE: The results are displayed in the “Output” file. For these analyzes a Mann-U-Whitney test is performed.

8.12. Include the result of the nonparametric test in the box plot of the exploratory data analysis.

8.13. Save the files by selecting **File** in the menu bar and choosing **Save**.

#### **REPRESENTATIVE RESULTS:**

Following cell delivery via the two approaches, the viability of cells delivered through the WN ( $97.2 \pm 2\%$ ,  $n=10$ ,  $p<0.002$ ) was higher when compared to injections by WJ using the E60-10 settings ( $85.9 \pm 0.16\%$ ,  $n=12$ ) (**Figure 2**). Biomechanical assessment results showed that: WN injections of cells in capture fluid displayed no significant difference with respect to the elastic moduli (EM; 0.992 kPa) when compared to the controls (1.176 kPa; **Figure 3A**), while WJ injections triggered a significant reduction of the cellular EM (0.440 kPa,  $p<0.001$ , **Figure 3B**). A decrease of 40 - 50% of the EM after WJ injections was noted. Even though, WN injections in cadaveric urethra tissue yielded no significant difference in cellular EM (**Figure 4A**) a significant reduction in EM was noted after WJ injections in tissue samples (0.890 kPa to 0.429 kPa;  $p<0.00$ , **Figure 4B**). Thus, absolute EM values after WJ injection were thereby reduced by 51%. Collectively, the results show that while WJ cell delivery fulfills an absolute requirement for a clinical implementation where more than 80% viable cells post delivery<sup>18</sup>, post WJ delivery the cell elastic moduli are affected. A lower cellular EM might facilitate the migration of features of the cells after WJ delivery. In such a wider distribution and range of regenerative capacities in the desired region<sup>19</sup>.

#### **FIGURE AND TABLE LEGENDS:**

**Figure 1. Anatomy of porcine bladder and urethra and injection sites.** A) The ventral side of the porcine bladder and urethra with the three ligaments fixing the bladder in the abdominal and pelvic cavity are shown. Additionally, the ureters that end on the dorsal side of the bladder are shown. B) Representative image of the cadaveric urethra used for WJ and WN injection. Longitudinally, the dorsal opened urethra with injection domes circled in black are shown.

**Figure 2. Cellular viability determination injections via WN and WJ.** pADSCs injected via WN or WJ were collected after injection and counted via Trypan exclusion to determine the viability. The cellular viability was significantly reduced after WJ injection when compared to cells delivered via WN. \*\*\*  $p<0.001$ . The data is graphically displayed as mean with standard deviation. Abbreviations: WJ – waterjet, WN – Williams needle. Figure adapted from Danalache et al. 2021<sup>19</sup>.

**Figure 3. Comparison of the quantified Young’s moduli of WN respectively WJ delivered cells into capture media and their corresponding controls.** No notable difference in EM was observed in the boxplots for the control (untreated) cell monolayers and WN delivered cells (**A**). Contrastingly, a significant decrease in elasticity can be noted between the boxplots of the

control cells and the WJ group (**B**). ns – not significant,  $p > 0.05$ , \*\*\* $p < 0.001$ . Abbreviations: WJ – waterjet, WN – Williams needle. Figure adapted from Danalache et al. 2021<sup>19</sup>.

**Figure 4. Comparison of the quantified Young's moduli of WN respectively WJ delivered cells into cadaveric urethra and their corresponding controls.** No notable difference was observed between cells delivered via WN cells and their corresponding controls (**A**). A significant decrease in elasticity was noted between the WJ delivered cells and the control cell monolayer (**B**). ns – not significant,  $p > 0.05$ , \*\*\* $p < 0.001$ . Abbreviations: WJ – waterjet, WN – Williams needle. Figure adapted from Danalache et al. 2021<sup>19</sup>.

**Table 1. Approach parameters.**

**Table 2. Run parameters.**

## DISCUSSION:

In the present study, we demonstrated and presented a step-by-step approach for WJ cell delivery procedure and employed a sequela of quantitative investigations to assess the effect of WJ delivery on cellular characteristics: cellular viability and biomechanical features (i.e., EM). Following WJ injection, 85.9% of the harvested cells were viable. In terms of WN injection, 97.2% of the cells retained their viability after injection. Thus, the WJ approach fulfills an absolute requirement for a clinical implementation: more than 80% viable cells post delivery<sup>18</sup>. While a standardized and reproducible protocol is achieved with the WJ approach, the outcome of needle injection delivery is highly dependent on the size and nozzle of the syringe and needle, pressure, flow rate and the physician performing the injection themselves<sup>19</sup>.

Studies employing WJ cell delivery in living animal models showed that by varying ejection pressure, the penetration depth can be adapted to the targeted tissue and as such, to the desired clinical application<sup>13,16</sup>. Transurethral cell injections in living animals under visual control reported misplacement or loss of cells in about 50% of animals treated<sup>20</sup>, while WJ injections reported precise cell injection rates above 90% (Linzenbold et al.<sup>16</sup> and unpublished observation). The current golden standard for cell delivery (needle injections) require penetration of the cannula in a targeted tissue. Therefore, needle cell translation causes injury and trauma in all cases. In the urethra, this may actually cause inflammation and toxification due to germ and toxins found in even in healthy urine. Additionally, the user-operation time in WJ injection is significantly shorter when compared to a needle injection: cells are placed within milliseconds into the intended tissue layer by presetting the pressure levels. In contrast, penetration depth on needle injection in remote areas by endoscopy is dependent on the skills and experience of the surgeon. The reproducibility of WJ injection is also expected to be superior, but presently only pre-clinical data exist<sup>15,16,20</sup> and less than 200 animals were investigated. In our recent study we noted that cellular elasticity is reduced by WJ application when compared to needle injections<sup>21</sup>. This can be attributed to the shear stress of cells in higher velocity during WJ delivery. Moreover, eventual cell loss might be compensated by a higher precision of cell placement and ejection within the region of interest as achieved with WJ guided delivery by visual guided cystoscopy<sup>22</sup>.

It is well known that mechanical forces direct stem cell behavior, regeneration potential as well as their subsequent viability and functionality post-transplantation<sup>10,23</sup>. The advent of atomic AFM provided a powerful tool for quantifying the mechanical properties of single living cells in nano scale resolution in aqueous conditions<sup>24,25,26,27</sup>. AFM is a reliable and highly sensitive method that can detect and record stiffnesses ranging from less than 100 Pa to 10<sup>6</sup> Pa, thus covering a wide range for the majority tissues and cells<sup>28</sup>. In fact, cell mechanics is emerging as label-free biomarker for evaluating cell state and in both physiological and pathological state<sup>29</sup> and cell elasticity is the synergetic and cumulative response of the nucleus - cytoskeleton crosstalk. It is well established that when a cell is subjected to external forces, these forces are transmitted from the plasma membrane via the cytoskeleton to the nucleus, resulting in intra-nuclear deformations and reorganization<sup>30-32</sup>. Therefore the nucleus, long seen as the genomic material and transcription apparatus, is a key player in the cellular mechanotransduction as well<sup>32</sup>. In fact, the importance of nuclear mechanics and nucleo-cytoskeletal connections, in all cellular functions and mutations, in lamins and linkers of the nucleo-skeleton to the cytoskeleton (LINC) complex - are at the onset foundation of several pathologies<sup>33,34</sup>. These forces could also indicate cellular artifacts. Specifically, external generated forces actually propagate along cytoskeletal filaments and are further transmitted to the nuclear lamina across the LINC complex; in response to these forces, the nucleus, in fact, becomes stiffer<sup>35,36</sup>, thus merging the two closely intertwined and connected processes. This is also the rationale of our approach and our nuclear mechanics measurements. Moreover, a precise placement of the cantilever on top of the nuclear surface also ensures a high degree of reproducibility and reduces variations owing to cell heterogeneity and attachment to the substratum.

Even though cell elasticity is emerging as label-free biomarker for evaluating the cell state and in both physiological and pathological states<sup>29</sup>, the measured elastic moduli are marked by large variations even in the same cell type<sup>37</sup>. A method to counteract such variations as suggested by Schillers et al. is the implementation of standardized nanomechanical AFM procedures (SNAP) that ensure a high reproducibility and applicability of elasticity measurements as a reliable quantitative marker to cells in various states<sup>38</sup>. Also, even though experimental parameters employed in the AFM analyses, such as indentation velocity, indenter shape and size as well as accurate representation of tip geometry in model fitting<sup>39</sup>, influence the absolute measured values<sup>40,41</sup>, these parameters should not impact the results within one study or a measured tendency.

However, bear in mind that AFM indentations are restricted to the analysis of the outer surface of cells and are, thus, incapable of scanning the inside of a cell membrane or particular intracellular structures. Usukura et al. proposed a "unroofing" method that breaks the cellular membrane and removes the cytoplasmic-soluble components<sup>42</sup>, thus allowing AFM- intracellular investigations. In our study, however, the focus was placed on the assessment of average elastic moduli rather than probing distinct and selective intracellular components.

Collectively, the consistency and reliability of the yielded AFM data strongly depends on the technical experience of the respective operator and could be biased by biological variability<sup>38</sup>. Accounting for all the sensitive variables that might affect the actual AFM results, the absolute

elastic values reported in this study cannot be generalized and are rather specific for our experimental setup.

Overall, our study provides evidence<sup>21</sup> as well as a step-by-step protocol for the superiority of WJ injections over needle injections for regenerative cell therapy regimen.

#### ACKNOWLEDGMENTS:

We thank our co-authors from the original publications for their help and support.

#### DISCLOSURES:

The authors J.K., M.D, T.A., A.S., W.K. A. have nothing to disclose. The authors W.L. and M.D.E. are employees of ERBE Medizintechnik Lt. Tübingen, the producer of the ERBEJet2 and the WJ prototype employed in this study.

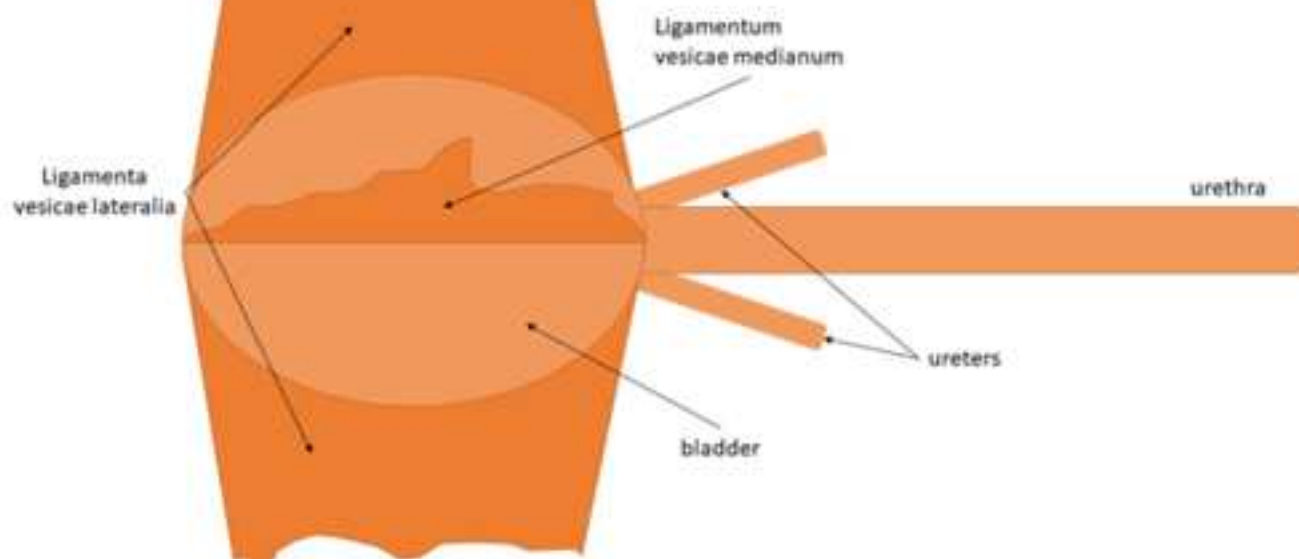
#### REFERENCES:

- 1 Milsom, I. *et al.* Global prevalence and economic burden of urgency urinary incontinence: a systematic review. *European Urology*. **65** (1), 79-95 (2014).
- 2 Lee, J. Y. *et al.* The effects of periurethral muscle-derived stem cell injection on leak point pressure in a rat model of stress urinary incontinence. *International Urogynecology Journal and Pelvic Floor Dysfunction*. **14** (1), 31-37; discussion 37 (2003).
- 3 Tran, C., Damaser, M. S. The potential role of stem cells in the treatment of urinary incontinence. *Therapeutic Advances in Urology*. **7** (1), 22-40 (2015).
- 4 Fu, Q., Song, X. F., Liao, G. L., Deng, C. L., Cui, L. Myoblasts differentiated from adipose-derived stem cells to treat stress urinary incontinence. *Urology*. **75** (3), 718-723 (2010).
- 5 Corcos, J. *et al.* Bone marrow mesenchymal stromal cell therapy for external urethral sphincter restoration in a rat model of stress urinary incontinence. *Neurourology and Urodynamics*. **30** (3), 447-455 (2011).
- 6 Smaldone, M. C., Chen, M. L., Chancellor, M. B. Stem cell therapy for urethral sphincter regeneration. *Minerva Urologica e Nefrologica*. **61** (1), 27-40 (2009).
- 7 Perin, E. C., López, J. Methods of stem cell delivery in cardiac diseases. *Nature Clinical Practice Cardiovascular Medicine*. **3 Suppl 1**, S110-113 (2006).
- 8 Zhang, M. *et al.* Cardiomyocyte grafting for cardiac repair: graft cell death and anti-death strategies. *Journal of Molecular and Cellular Cardiology*. **33** (5), 907-921 (2001).
- 9 Amer, M. H., White, L. J., Shakesheff, K. M. The effect of injection using narrow-bore needles on mammalian cells: administration and formulation considerations for cell therapies. *Journal of Pharmacy and Pharmacology*. **67** (5), 640-650 (2015).
- 10 Amer, M. H., Rose, F. R. A. J., Shakesheff, K. M., Modo, M., White, L. J. Translational considerations in injectable cell-based therapeutics for neurological applications: concepts, progress and challenges. *NPJ Regenerative Medicine*. **2**, 23-23 (2017).
- 11 Linzenbold, W., Fech, A., Hofmann, M., Aicher, W. K., Enderle, M. D. Novel Techniques to Improve Precise Cell Injection. *International Journal of Molecular Sciences*. **22** (12), 6367 (2021).
- 12 Adamo, A., Roushdy, O., Dokov, R., Sharei, A., Jensen, K. F. Microfluidic jet injection for delivering macromolecules into cells. *Journal of Micromechanics and Microengineering: Structures, Devices, and Systems*. **23**, 035026 (2013).

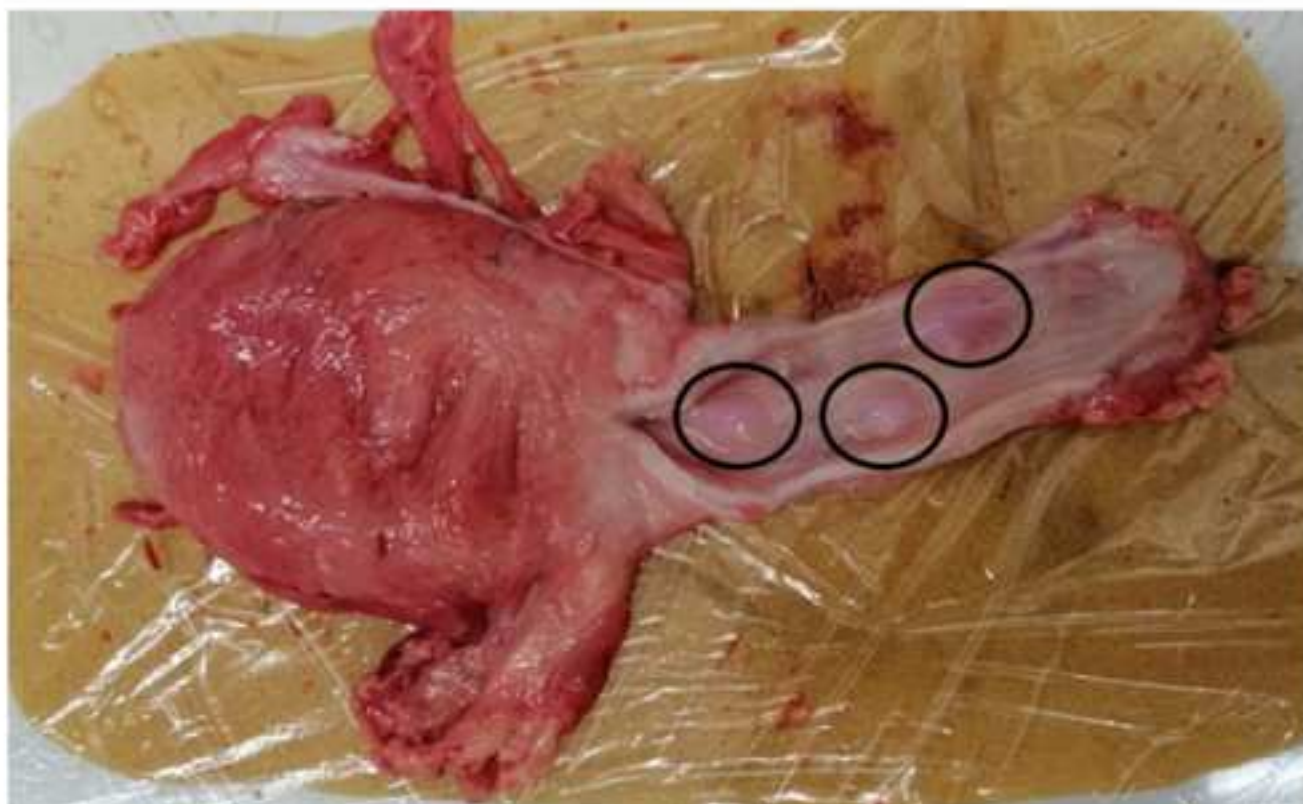
661 13 Jäger, L. *et al.* A novel waterjet technology for transurethral cystoscopic injection of viable  
662 cells in the urethral sphincter complex. *Neurourology and Urodynamics*. **39** (2), 594-602 (2020).  
663 14 Weber, M. *et al.* Hydrojet-based delivery of footprint-free iPSC-derived cardiomyocytes  
664 into porcine myocardium. *Scientific Reports*. **10** (1), 16787 (2020).  
665 15 Jäger, L. *et al.* A novel waterjet technology for transurethral cystoscopic injection of viable  
666 cells in the urethral sphincter complex. *Neurourology and Urodynamics*. **39** (2), 594-602 (2020).  
667 16 Linzenbold, W. *et al.* Rapid and precise delivery of cells in the urethral sphincter complex  
668 by a novel needle-free waterjet technology. *BJU International*. **127** (4), 463-472 (2021).  
669 17 Danalache, M., Tiwari, A., Sigwart, V., Hofmann, U. K. Application of Atomic Force  
670 Microscopy to Detect Early Osteoarthritis. *Journal of Visualized Experiments*. (159),  
671 doi:10.3791/61041 (2020).  
672 18 Gálvez-Martín, P., Hmadcha, A., Soria, B., Calpena-Campmany, A. C., Clares-Naveros, B.  
673 Study of the stability of packaging and storage conditions of human mesenchymal stem cell for  
674 intra-arterial clinical application in patient with critical limb ischemia. *European Journal of*  
675 *Pharmaceutics and Biopharmaceutics*. **86** (3), 459-468 (2014).  
676 19 Danalache, M. *et al.* Injection of Porcine Adipose Tissue-Derived Stromal Cells by a Novel  
677 Waterjet Technology. *International Journal of Molecular Sciences*. **22** (8) (2021).  
678 20 Amend, B. *et al.* Precise injection of human mesenchymal stromal cells in the urethral  
679 sphincter complex of Göttingen minipigs without unspecific bulking effects. *Neurourology and*  
680 *Urodynamics*. **36** (7), 1723-1733 (2017).  
681 21 Danalache, M. *et al.* Injection of Porcine Adipose Tissue-Derived Stromal Cells by a Novel  
682 Waterjet Technology. *International Journal of Molecular Sciences*. **22** (8), 3958 (2021).  
683 22 Strasser, H. *et al.* 328: Transurethral Ultrasound Guided Stem Cell Therapy of Urinary  
684 Incontinence. *Journal of Urology*. **175** (4S), 107-107 (2006).  
685 23 Vining, K. H., Mooney, D. J. Mechanical forces direct stem cell behaviour in development  
686 and regeneration. *Nature reviews. Molecular Cell Biology*. **18** (12), 728-742 (2017).  
687 24 Ding, Y., Xu, G.-K., Wang, G.-F. On the determination of elastic moduli of cells by AFM  
688 based indentation. *Scientific Reports*. **7** (1), 45575 (2017).  
689 25 Charras, G. T., Horton, M. A. Single cell mechanotransduction and its modulation analyzed  
690 by atomic force microscope indentation. *Biophysical Journal*. **82** (6), 2970-2981 (2002).  
691 26 Carl, P., Schillers, H. Elasticity measurement of living cells with an atomic force  
692 microscope: data acquisition and processing. *Pflügers Archiv: European Journal of Physiology*. **457**  
693 (2), 551-559 (2008).  
694 27 Darling, E. M., Topel, M., Zauscher, S., Vail, T. P., Guilak, F. Viscoelastic properties of  
695 human mesenchymally-derived stem cells and primary osteoblasts, chondrocytes, and  
696 adipocytes. *Journal of Biomechanics*. **41** (2), 454-464 (2008).  
697 28 Thomas, G., Burnham, N. A., Camesano, T. A., Wen, Q. Measuring the mechanical  
698 properties of living cells using atomic force microscopy. *Journal of Visualized Experiments*. (76),  
699 50497 (2013).  
700 29 Li, M., Dang, D., Liu, L., Xi, N., Wang, Y. Atomic Force Microscopy in Characterizing Cell  
701 Mechanics for Biomedical Applications: A Review. *IEEE Trans Nanobioscience*. **16** (6), 523-540  
702 (2017).  
703 30 Morimoto, A. *et al.* A conserved KASH domain protein associates with telomeres, SUN1,  
704 and dynactin during mammalian meiosis. *The Journal of Cell Biology*. **198** (2), 165-17 (2012).

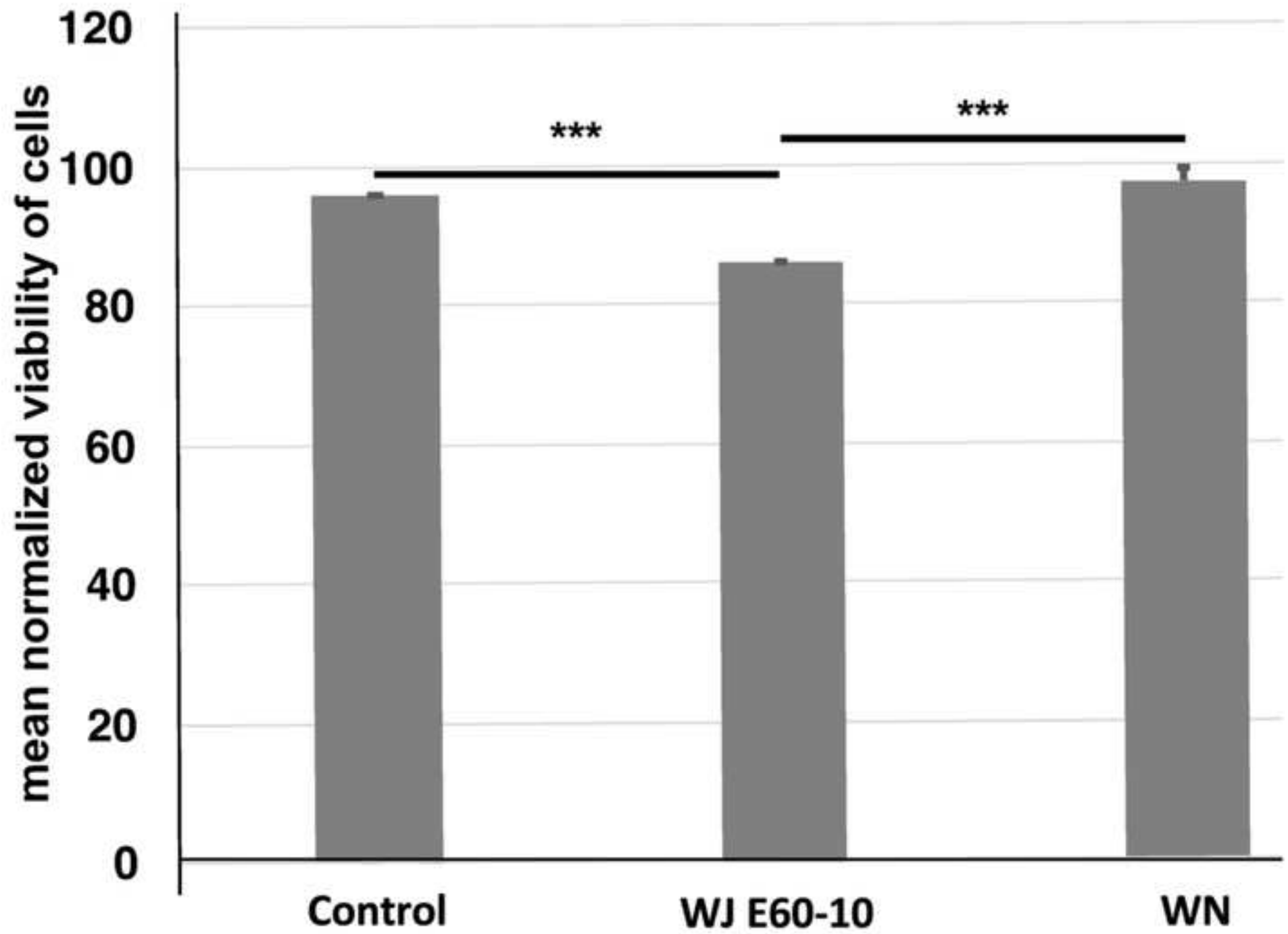
- 31 Lombardi, M. L. *et al.* The interaction between nesprins and sun proteins at the nuclear envelope is critical for force transmission between the nucleus and cytoskeleton. *Journal of Biological Chemistry*. **286** (30), 26743-26753 (2011).
- 32 Isermann, P., Lammerding, J. Nuclear Mechanics and Mechanotransduction in Health and Disease. *Current Biology*. **23** (24), R1113-R1121 (2013).
- 33 Méjat, A. LINC complexes in health and disease. *Nucleus*. **1** (1), 40-52 (2010).
- 34 Folker, E. S., Östlund, C., Luxton, G. G., Worman, H. J., Gundersen, G. G. Lamin A variants that cause striated muscle disease are defective in anchoring transmembrane actin-associated nuclear lines for nuclear movement. *Proceedings of the National Academy of Sciences*. **108** (1), 131-136 (2011).
- 35 Guilluy, C. *et al.* Isolated nuclei adapt to force and reveal a mechanotransduction pathway in the nucleus. *Nature cell biology*. **16** (4), 376-381 (2014).
- 36 Fischer, T., Hayn, A., Mierke, C. T. Effect of Nuclear Stiffness on Cell Mechanics and Migration of Human Breast Cancer Cells. *Frontiers in Cell and Developmental Biology*. **8**, 393-393 (2020).
- 37 Kuznetsova, T. G., Starodubtseva, M. N., Yegorenkov, N. I., Chizhik, S. A., Zhdanov, R. I. Atomic force microscopy probing of cell elasticity. *Micron*. **38** (8), 824-833 (2007).
- 38 Schillers, H. *et al.* Standardized Nanomechanical Atomic Force Microscopy Procedure (SNAP) for Measuring Soft and Biological Samples. *Scientific Reports*. **7** (1), 5117 (2017).
- 39 Costa, K. D., Yin, F. C. Analysis of indentation: implications for measuring mechanical properties with atomic force microscopy. *Journal of Biomechanical Engineering*. **121** (5), 462-471 (1999).
- 40 Stolz, M. *et al.* Dynamic elastic modulus of porcine articular cartilage determined at two different levels of tissue organization by indentation-type atomic force microscopy. *Biophysical Journal*. **86** (5) (2004).
- 41 Park, S., Costa, K. D., Ateshian, G. A., Hong, K. S. Mechanical properties of bovine articular cartilage under microscale indentation loading from atomic force microscopy. *Proceedings of the Institution of Mechanical Engineers, Part H*. **223** (3), 339-347 (2009).
- 42 Usukura, E., Narita, A., Yagi, A., Ito, S., Usukura, J. An Unroofing Method to Observe the Cytoskeleton Directly at Molecular Resolution Using Atomic Force Microscopy. *Scientific Reports*. **6** (1), 27472 (2016).

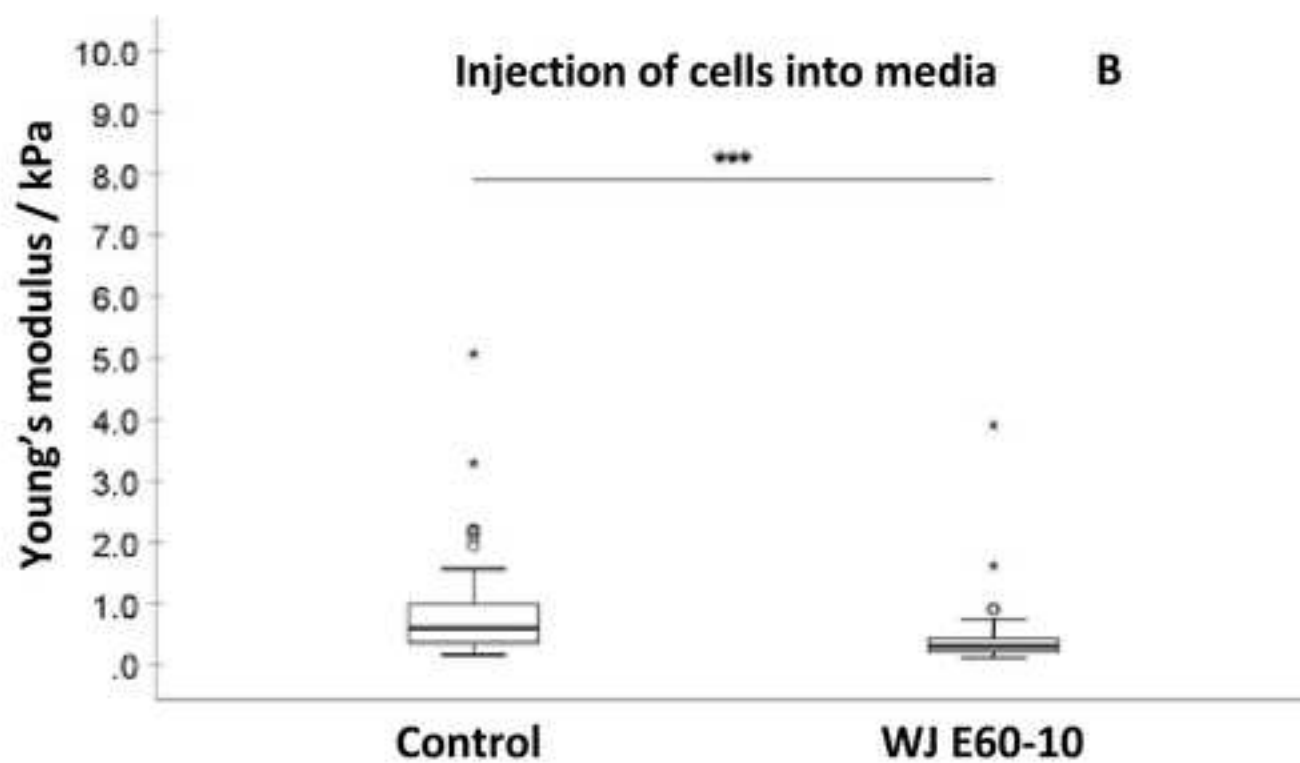
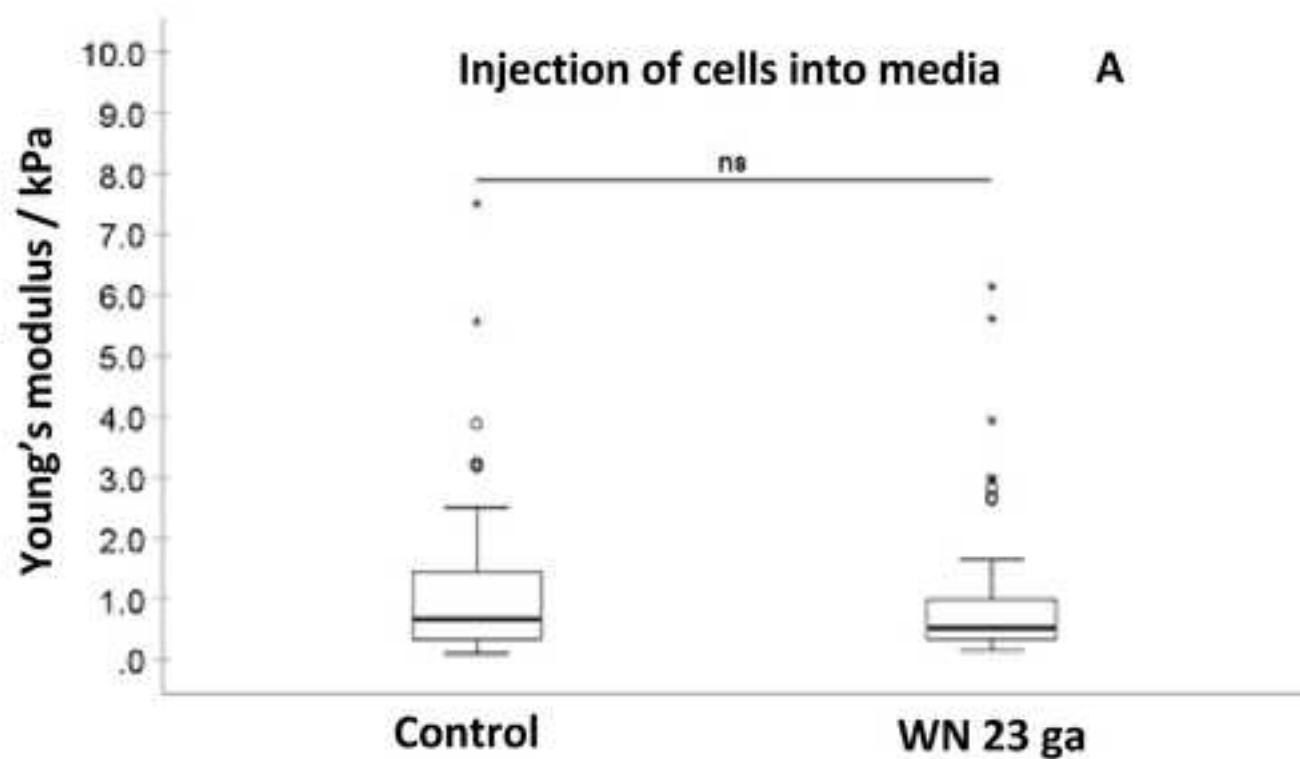
A

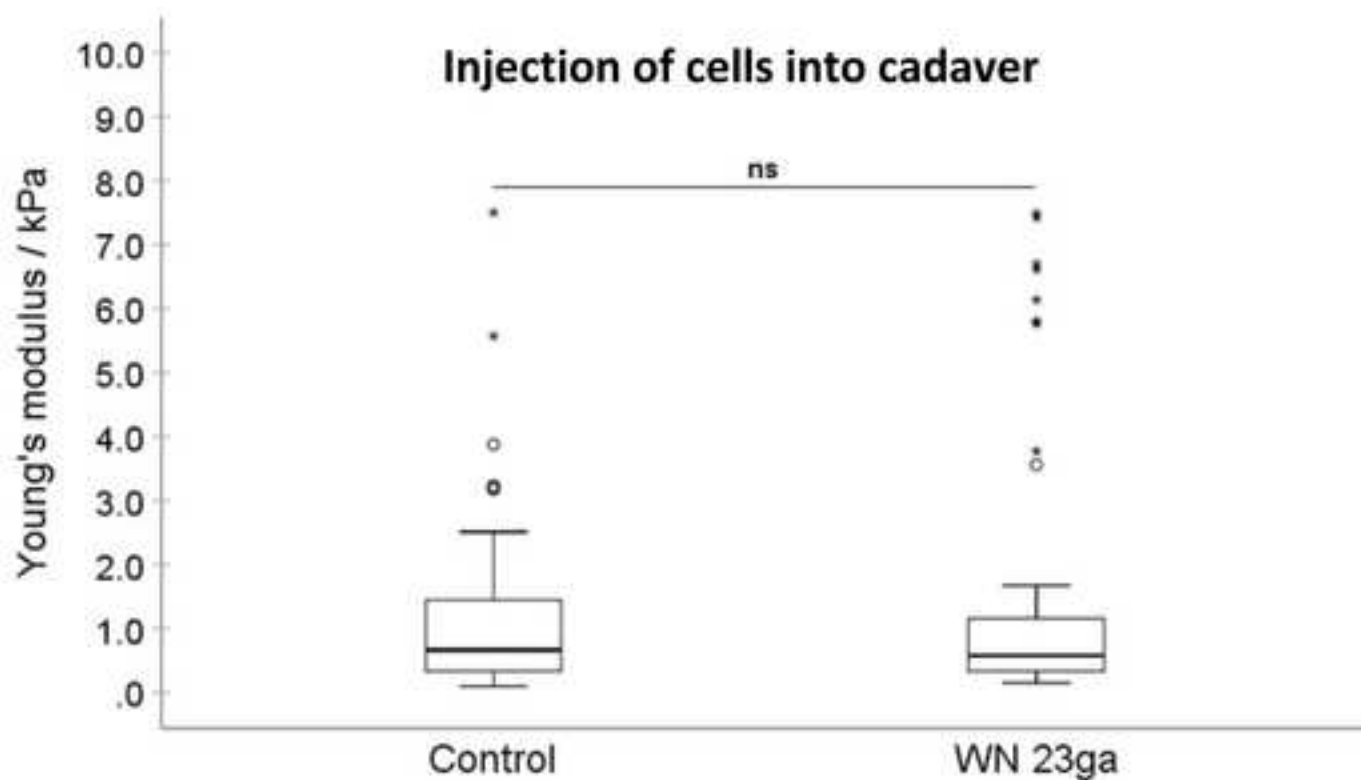
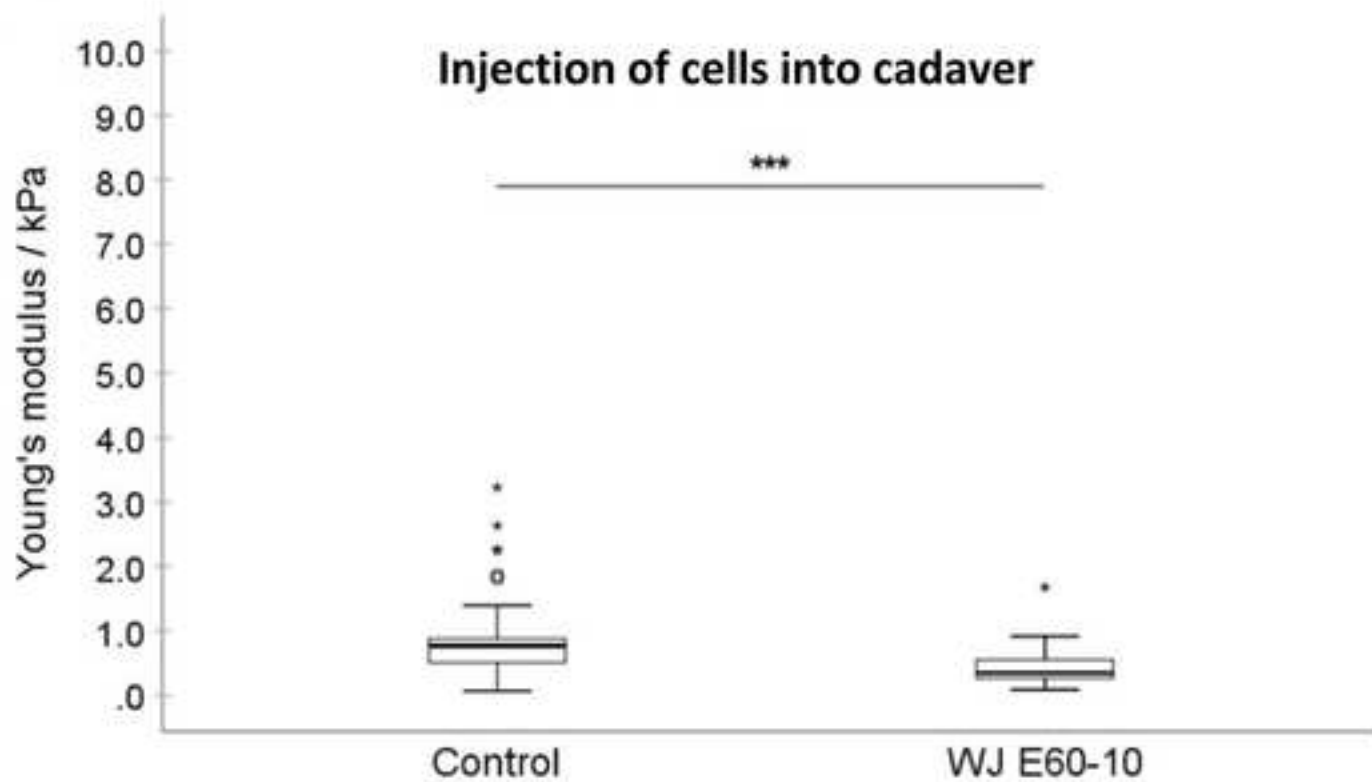


B







**A****B**

Approach parameter	Value
Approach IGain	3.0 Hz
Approach PGain	0.0002
Approach target height	10.0 μm
Approach setpoint	3.00 V
Approach baseline	0.00 V

Run parameter	Value
Set point	10 nN
Z Movement/ Extend Speed	Constant speed/ 5.0 μm/s
Contact time	0.0 s
Pulling length	90 μm
Delay Mode	Constant Force
Sample rate	2000 Hz



Click here to access/download  
**Table of Materials**  
**Materials.xlsx**

**Point to point response file manuscript number: JoVE63132**

**Injection of porcine adipose tissue-derived stroma cells via waterjet technology**

**AUTHORS AND AFFILIATIONS:**

Jasmin Knoll<sup>1\*</sup>, Marina Danalache<sup>2\*</sup>, Walter Linzenbold<sup>3</sup>, Markus Enderle<sup>3</sup>, Tanja Abruzzese<sup>1</sup>, Arnulf Stenzl<sup>1</sup>, Wilhelm K. Aicher<sup>1#</sup>

<sup>1</sup> Department of Urology, University Hospital Tübingen, Tübingen, Germany

<sup>2</sup> Department of Orthopaedic Surgery, University Hospital Tübingen, Tübingen Germany

<sup>3</sup> ERBE Elektromedizin GmbH Tübingen, Germany

\*Both authors contributed equally

**# Corresponding Author:**

Prof. Dr. Wilhelm K. Aicher (aicher@uni-tuebingen.de)

**Email Addresses of Co-Authors:**

Jasmin Knoll	(jasmin.knoll@med.uni-tuebingen.de)
Marina Danalache	(marina.danalache@med.uni-tuebingen.de)
Walter Linzenbold	(Walter.Linzenbold@erbe-med.com)
Markus Enderle	(Markus.Enderle@erbe-med.com)
Tanja Abruzzese	(Tanja.Abruzzese@med.uni-tuebingen.de)
Arnulf Stenzl	(Urologie@med.uni-tuebingen.de)
Wilhelm K. Aicher	(aicher@uni-tuebingen.de)

Date: 19.09.2021

Author's response to reviews: [printed in blue](#)

**Editorial comments:**

Changes to be made by the Author(s):

1. Please take this opportunity to thoroughly proofread the manuscript to ensure that there are no spelling or grammar issues.

We apologize for the inconvenience. As suggested, we have made the required language adjustments and corrections.

2. Please clarify the corresponding author for this study as the names are different in the Editorial Manager and the main manuscript.

The corresponding author is Prof. Aicher as indicated in the manuscript.

3. Please revise the following lines to avoid previously published work: 63-64, 71-76, 481-483.

The indicated lines were rephrased as suggested.

4. Line 79: The superscript 88 seems to be a typographical error. Please correct this.

The superscript was removed as indicated by the editor.

5. Please revise the text to avoid the use of any personal pronouns (e.g., "we", "you", "our" etc.).

Changes made as indicated by the editor.

6. Please revise the Introduction to include all of the following:

We do acknowledge this valid remark raised by the editor. We do, however, have to spell out that WJ is a novel approach cell delivery that is currently present as a prototype.

(a) A description of the context of the technique in the wider body of literature

We have added additional information and also spelled out the fact that although the WJ is a novel approach, it is still at a prototype stage.

(b) Information to help readers to determine whether the method is appropriate for their application.

As suggested we have included additional information with respect to the technique applicability and suitability.

7. Please use SI units as much as possible and abbreviate all units: L, mL,  $\mu$ L, cm, kg, etc. Use h, min, s, for hour, minute, second.

We have adjusted all unit abbreviations.

8. Please add more details to your protocol steps. Please ensure you answer the “how” question, i.e., how is the step performed?

As suggested we added to the mentioned steps some more information.

Step 1.6: Was the aspiration done with a pipette or an aspirator? Please specify.

The aspiration was performed with a pipette. It was adjusted accordingly in the protocol.

Step 1.7: Please specify the filtration membrane.

The filtration membrane was specified as suggested.

Step 1.11, Note: In how many flasks were the cells seeded in this protocol. How do you determine this: is it by the size of the pellet or its density or anything else? Please specify.

As already mentioned in the protocol the number of flasks depends on the size of the cell pellet.

Step 2.9, 5.2, 6.2, 7.1.1: Please denote the cell number as  $3 \times 10^5$ ,  $2.4 \times 10^6$ ,  $6 \times 10^6$ ,  $5 \times 10^5$

The cell numbers were adjusted as required.

Step 3.6: What was used here: a microscope or flow cytometry? Please elaborate on the steps for using the instrument. If this step needs to be filmed, please make sure to provide all the details such as “click this”, “select that”, “observe this”, etc. Please mention all the steps that are necessary to execute the action item. Please provide details so a reader may replicate your analysis including buttons clicked, inputs, screenshots, etc. Please keep in mind that software steps without a graphical user interface (GUI) cannot be filmed. Also, please mention any other parameter or image settings. Please ensure that in the software steps, all the button clicks are bolded.

All steps necessary to replicate this process were included in the manuscript.

Step 4.4: Please specify the cut dimension.

No cutting was done. The term “cut” was corrected.

Step 5.2, 6.2: Are the authors referring to step 2.9 because the cell density is mentioned in that step. There is no cell density in step 4.2. Are the authors referring to step 5.2? Please proofread the manuscript thoroughly.

Yes, this suggestion was correct. We apologize for the inconvenience. The corrections were adjusted in the protocol.

Step 5.10, 6.10: How was this done? Please provide all steps associated. Alternatively, add references to published material specifying how to perform the protocol action.

Steps were added as suggested.

Step 6.5: Please elaborate the steps for using the instrument.

The exact operation of the prototype cannot be disclosed as we have to comply with the confidentiality agreement with our industry partner.

Step 7: Please provide the commands/clicks in bold letters with the initial letter capitalized.

The changes were implemented in the revised manuscript.

Step 7.4: Please provide details as to how the data was processed and the various steps or commands used to analyze and plot the data. Alternatively, add references to published material specifying how to perform the protocol action.

We have included additional text and reference our previously published manuscript describing this step more in depth.

9. Please provide volume and concentration of reagents/media/solution used. For example, PBS, Trypsin-EDTA, growth media, etc.

The composition of the growth media was added in step 1.4.1.

Volumes were added in step 1.11, 2.2, 3.1, 3.5, 5.9, 6.9, 7.1.3,

Concentration of Trypsin-EDTA was added in step 2.3.

10. Please remove the embedded figure(s) from the manuscript.

As suggested we removed the embedded figures from the manuscript.

11. Please remove the embedded Table from the manuscript. All tables should be uploaded separately to your Editorial Manager account in the form of an .xls or .xlsx file. Each table must be accompanied by a title and a description after the Representative Results of the manuscript text.

We removed the Table from the manuscript. However, we have to point out that Table1 is part of the protocol section and it is in fact not depicting any results.

12. Please highlight up to 3 pages of the Protocol (including headings and spacing) that identifies the essential steps of the protocol for the video, i.e., the steps that should be visualized to tell the most cohesive story of the Protocol and it should also be in line with the Title of the manuscript. Remember that non-highlighted Protocol steps will remain in the manuscript, and therefore will still be available to the reader.

We have highlighted 3 pages of protocol.

13. Figure 2: Please describe what the error bar stands for: standard error or standard deviation, in the figure legend?

We thank the editor for highlighting this aspect. Additional information has been added in the Figure's legend.

14. Figure 3: What does ns stand for? Please specify in the figure legend

'ns' stands for not significant. We have included this information in the figure legend.

15. As we are a methods journal, please revise the Discussion to explicitly cover the following in detail in 3-6 paragraphs with citations:

- (a) Critical steps within the protocol
- (b) Any modifications and troubleshooting of the technique
- (c) Any limitations of the technique
- (d) The significance with respect to existing methods
- (e) Any future applications of the technique

16. Please ensure that the Representative Results explain the context of the technique you have described, e.g., how do these results show the technique, suggestions about how to analyze the outcome, etc. The Results section should focus on the effectiveness of your technique backed up with data.

As indicated we have rewritten the entire discussion section and focused of the techniques and their advantages and limitations.

17. Please do not abbreviate journal names in references. Article titles should start with a capital letter, end with a period, and appear exactly as they were published in the original work, without abbreviations or truncations.

We have adjusted the references accordingly.

**Reviewer #1:****Manuscript Summary:**

Authors present a method of cell injection via needle free waterjet technology in detail and cellular elasticity measurement with AFM. The presentation is very precise and understandable.

**Major Concerns:**

1. Although cell viability is not significantly lower, but viability via WJ is lower than normal and WN. What do you think is the reason?

We thank the reviewer for raising this point. Mechanical stress balance the lower viability vs the surgical advantages which yielded significantly less misplacement i.e. 95% of samples investigated were found in the targeted tissue (unpublished data) whereas WN yielded misplacement in about 50% of samples investigated<sup>1</sup>

2. The authors said they measured cell elasticity above the cell nucleus. However, cell elasticity is primarily determined by F-actin, a predominantly present membrane, not the nucleus. Why did you measure the elasticity above the nucleus?

We acknowledge the reviewer's remark, which we gladly like to elaborate. While we do agree with the reviewer's comments that F-actin network is a key component, cell elasticity is, in fact, the synergetic and cumulative response of the nucleus - cytoskeleton crosstalk. It is well established that external forces applied to a cell are transmitted from the plasma membrane via the cytoskeleton to the nucleus, resulting in (intra-)nuclear deformations and reorganization<sup>2-4</sup>. Therefore the nucleus long seen as the genomic material and transcription machinery is a key player in the cellular mechanotransduction<sup>4</sup>. In fact, the importance of nuclear mechanics and nucleo-cytoskeletal connection in all cellular function and mutations in lamins and linkers of the nucleo-skeleton to the cytoskeleton (LINC) complex - are at the onset foundation of several pathologies<sup>5,6</sup>.

By making an analogy to our study design, external generated forces actually propagate along cytoskeletal filaments and are further transmitted to the nuclear lamina across the LINC complex and in response to these forces the nucleus in fact, becomes stiffer<sup>7</sup>. Moreover, cytoskeletal mechanics are in fact regulated by nuclear mechanics such as nuclear stiffening<sup>8</sup>, thus making the two closely intertwined and connected processes. This is also the rationale behind our approach and implicitly of our nuclear measurements.

Furthermore, also advocating for our nucleus measurements - we precisely placed the cantilever on top of the nuclear surface to ensure a high degree of reproducibility and reduce variation owing to cell to cell variation.

In the revised version of the manuscript, particularly in the Discussion section, we have added additional information.

**Reviewer #2:****Manuscript Summary:**

The manuscript presents a step-by-step protocol for obtaining and culturing porcine adipose tissue-derived stromal cells, preparation urethral tissue to be injected with pADSC, accompanied by detailed procedure of their injection. Each step is described in details, however, some important information is missing (as

listed below). To certain extent it is obvious for researcher working with cells but the manuscript should present all steps that will allow to reproduce the protocol in each laboratory also by beginners. Especially, AFM part should be strongly revised and free of errors.

We thank the reviewer for the time invested to help to improve our manuscript, and we do acknowledge that based on his/her comments our manuscript has improved considerably. While we appreciate the reviewer's concerns, we do have to state that we have previously published the AFM section. This part has been already presented in our previous publications (please Danalache et al 2020&2021: doi: 10.3791/61041 and doi.org/10.3390/ijms22083958).

#### Major Concerns:

The following information must be included:

1) please describe the culture media composition

The composition of the culture media was added in step 1.4.1.

2) please describe whether antibiotics have to be used in cell culture

We included this description in the composition of the media.

3) please indicate what is the concentration of trypsin-EDTA solution (depending on cell type various concentrations are used)

The concentration of Trypsin-EDTA was added in the protocol.

4) please describe why red fluorescent is applied

PI staining was employed in order to discriminate dead cells from viable cells after injections. To eliminate apriori dead cells from cells that died after injection.

5) please use one term (culture media or growth media)

The terms were adjusted accordingly.

6) AFM measurements - time of incubation is not sufficient. Typically, in the AFM cells are measured after 24 hours.

We thank the reviewer for this remark, we do however have to state that in order to avoid variances due to cells in G1 phase and during mitosis (which has significant effects on cell mechanics) we focused on conducting the AFM measurements exactly 3 h after seeding cells. We have included this missing information in our protocol. In fact, in a preliminary study, we actually determined the optimal time required for 50% of cells to attach - that is 3 h. We further used this time point for all of our

measurements in order to also avoid possible artifacts triggered by the spreading of cells attached to stiff polystyrene cell culture flasks.

A step controlling the morphology of the cells should be added. Mechanical properties of cells of the same morphology should be compared. Otherwise, the obtained difference can be related to spreading dynamics.

The morphology of the cells was analyzed, please check the original publication (Danalache et al.<sup>9</sup> – Figure 1), and yes - cells with a similar morphology were subjected to investigations. With respect to the spreading dynamics considerations as beforehand mentioned the cells were measured 3 h after seeding the cells to counteract the possible artifacts caused by the spreading of cells onto stiff polystyrene cell culture flasks.

7) The type of the cantilever has to be mentioned (spherical or pyramidal). What means tip A?

We thank the reviewer for this remark. In line with the journal's format, cantilever specifications as well information with respect to the AFM device, etc. are present in a separate .xls. file called "Tables for materials". All of the technical specifications are also presented in this table.

8) Cantilever calibration have to be precisely described (see paper Schillers et al. Sci. Rep. 7 (2017) 5117).

We thank the reviewer to raising this point. The calibration of the cantilever was done following the same parameters and step as indicated in our previous publication on the topic: doi: 10.3791/61041. We have added this information in our revised protocol: Step 7.2.15, Line 449 - 450. We thank the reviewer for his/her literature suggestion. After careful examination we have now included it in our manuscript - specifically in the Discussion section where we address the advantages and limitations of AFM measurements.

9) The authors have to be precise in describing the cantilever. Cantilever is a flexible (rectangular or triangular) level with the pyramidal or spherical tip mounted and its free end. Thus, the laser beam deflects from the back side of the cantilever.

We thank the reviewer for this remark, however we are not sure how to address it. We have included all information and technical data of the cantilever we used in "Table of Materials". If the reviewer still considers that additional information is required we can gladly incorporate it.

10) It is not clear what means "Adjust the AFM head on the AFM device" - 7.2.5. From the text, I would guess the authors mount the AFM head.

We thank the reviewer for this valid point, the text has now been adjusted.

11) Approach parameters vary depending on the AFM instruments used. IGain and PGain are specific for each AFM as they are linked with the specific controller. Target height ? Why it is 10 micron? Approach

set point 3V can denote 5 nN or 0.5 nN depending on the calibration. How much force (or deflection expressed in nm) can be applied?

We thank the reviewer for raising this point. A comprehensive, detailed protocol on the AFM setup and step to step calibration (including calibration parameters) using our device has been already presented in our previous JoVE publication: please see doi: 10.3791/61041. We have also clearly indicated this reference in our manuscript, Line: 449-450. And of course several parameters such as IGain and PGain, etc. are specific for our device as the present protocol is meant to show to AFM operation with our technique and device, this also means that this is a generalized approach but rather a specific one for our study design. We clearly delineated this aspect in our Discussion, the text runs: "Considering all the sensitive variables that might affect the actual AFM measurement results, the absolute elastic values reported in this study cannot be generalized and are rather specific for our experimental setup."

12) It is important to mentioned whether close loop has to be on or off.

We thank the reviewer for the remark. We always used the close loop control (i.e.: the feedback from the capacitive sensors is on). Experiments can be performed either in "constant height" or "constant force" mode and in our present study we conducted our experiments in "constant force" mode. We have added additional information to our protocol section, Step 7.2.12, Line 440.

13) RUN parameters. Again, 1 V can denote 0.1 nN or 1 nN or 10 nN depending on the calibration. This should be clarified. Too much force will destroy sample while too low force probes only surface corrugations. It would be difficult to get the information on mechanical properties of cells.

We do appreciate the time and effort invested by the reviewer and we acknowledge all of the points raised by the reviewer. We guess the misunderstanding lies in fact that the AFM technique and operational steps was already published by our group (doi: 10.3791/61041) and in the present protocol we just cited and indicated initial publication without elaborating the individual steps. We went for this approach in order to avoid duplication and self-plagiarism. We have also now included a new "**Table 2**" with the exact RUN parameters we employed.

14) Calibration must be performed before the sample measurements. Based on calibration RUN parameters can be defined.

We agree with the reviewer on this point and indeed the calibration is an absolute requirement that has to be done prior to the actual measurements. And, yes - following the calibration the "Run" measurements were identified. All these points are presented in a sequential fashion in our previous publication (doi: 10.3791/61041), which we also clearly referenced in our protocol. We did not elaborate the steps that were previously presented and published, we just indicated the corresponding reference in our protocol.

15) Elasticity measurements. It is not clear where to measure, how much force has to be applied to the cells

Following the calibration step, the cells were visually identified and focused (please also see the original publication on which this protocol is based on: doi.org/10.3390/ijms22083958; in particular Figure 9:

“Representative images indicating the regions of interest subjected to elasticity measurements via AFM”). Then then computer mouse was placed at the middle of the cell , above the nucleus. The AFM tip was then focus on, moved and positioned directly above the cell nucleus exactly where the mouse cursor was initially placed. We used the computer mouse as visual marker to identify the target site of indentation, followed by the actual measurements. In the revised version of the protocol, these steps are indicated together with the parameters we used (Table 2, Section 7.3, lines 452 - 466).

16) What is the indentation depth used for the Young's modulus determination. Depending on the load force the modulus value will be different as cells are not fully elastic and isotropic.

We thank the reviewer for the remark, the elasticity of the cells was quantified at the indentation depth of 0.4  $\mu\text{m}$ .

17) The protocol how to calculate the elastic modulus has to be included. What about tilt corrections?

The calculation of the Young's modulus from the generated force curves using the Hertz fit model was also presented in our previous Jove publication: doi: 10.3791/61041. This information has now been added to the protocol section, Line 469-470, Step 7.4.1.

18) What kind of statistical tests are used to quantify the statistical significance?

As indicated by the reviewer, an additional section detailing the statistical analysis was included in the revised version of the protocol.

In the protocol, the relativeness of Young's modulus has to be discussed together with applicability of Hertz contact mechanics. Apart from this short discussion, citing one or two references from the groups working on cell or tissue mechanics AFM for at least one decade would be beneficial. In that manner, the reader will be aware of all drawbacks linked with the use of AFM to quantify biomechanical properties of living cells.

We knowledge the reviewers remark and we have rewritten the entire discussion sections as to focus on the experimental approach discussing the advantages and limitations.

There is also no verification method described. The differences between all groups of cells can be obtained if measurements are performed using the same cantilever under the condition that spring constant and photodetector sensitivity remains more or less constant.

We appreciate the concern; however, we have to state that this was indeed the case - for all of the measurements we used the exact same cantilever, temperature, set point, calibration settings etc. This required great skill but in the same time represents an absolute requirement in order to be able to conduct interferential statistical analysis.

Minor Concerns:

Fig. 1 is not informative. Its integration with a histological image would be more valuable.

The image was adjusted with a picture of the injection domes in the opened urethra. A histological image is not possible to provide in this manuscript because no histological analyses were performed in this study. However, histological analyses were performed in previous studies<sup>10,11</sup>.

### **Reviewer #3:**

#### **Manuscript Summary:**

The manuscript describes in great details about a method to inject primary isolated cells using a needle free approach. The authors have used cadaveric tissues as a model and also characterized the post delivery aspects of cell viability as well as force measurements. It's a well written manuscript with great details.

#### **Major Concerns:**

None

#### **Minor Concerns:**

The details of homogenization must be provides, speed rpm etc.

As suggested by the reviewer we have added additional information with respect to the homogenization step to our revised version of the protocol.

Details of AFM model used and cantilevers are required

We thank the reviewer for this remark. In accordance with the journal format, the exact details of the AFM device as well as the cantilever employed (including technical details) are included in the additional .xls.file - "Table of Materials".

It would be good to observe the cells using a microscope before and after delivery. Where are they located in the tissue? and how long ?

We thank the reviewer for this remark, however we do have to state that the localization of the cells was not the aim of the present study. We in fact, extract the cells directly after transplantation. Prior to the actual delivery we labelled (Calcein staining) and visualized the cells ( please check the original publication on which this protocol is based: Danalache et al<sup>9</sup>, where we included also controls. Moreover in previous studies we actually addressed the point raised by the reviewer and analyzed the localization and distribution of injected cells (please see Jäger et al<sup>10</sup> and Linzenbold et al<sup>11</sup>). The present protocol aims to visually demonstrate the WJ methodological approach in a stepwise manner.

### **References**

- 1 Amend, B. *et al.* Precise injection of human mesenchymal stromal cells in the urethral sphincter complex of Göttingen minipigs without unspecific bulking effects. *Neurourol Urodyn.* **36** (7), 1723-1733, doi:10.1002/nau.23182, (2017).
- 2 Morimoto, A. *et al.* A conserved KASH domain protein associates with telomeres, SUN1, and dynactin during mammalian meiosis. *The Journal of cell biology.* **198** (2), 165-172, doi:10.1083/jcb.201204085, (2012).
- 3 Lombardi, M. L. *et al.* The interaction between nesprins and sun proteins at the nuclear

- envelope is critical for force transmission between the nucleus and cytoskeleton. *J Biol Chem.* **286** (30), 26743-26753, doi:10.1074/jbc.M111.233700, (2011).
- 4 Isermann, P. & Lammerding, J. Nuclear Mechanics and Mechanotransduction in Health and Disease. *Current Biology.* **23** (24), R1113-R1121, doi:<https://doi.org/10.1016/j.cub.2013.11.009>, (2013).
- 5 Méjat, A. LINC complexes in health and disease. *Nucleus.* **1** (1), 40-52 (2010).
- 6 Folker, E. S., Östlund, C., Luxton, G. G., Worman, H. J. & Gundersen, G. G. Lamin A variants that cause striated muscle disease are defective in anchoring transmembrane actin-associated nuclear lines for nuclear movement. *Proceedings of the National Academy of Sciences.* **108** (1), 131-136 (2011).
- 7 Guilluy, C. *et al.* Isolated nuclei adapt to force and reveal a mechanotransduction pathway in the nucleus. *Nature cell biology.* **16** (4), 376-381 (2014).
- 8 Fischer, T., Hayn, A. & Mierke, C. T. Effect of Nuclear Stiffness on Cell Mechanics and Migration of Human Breast Cancer Cells. *Frontiers in Cell and Developmental Biology.* **8** 393-393, doi:10.3389/fcell.2020.00393, (2020).
- 9 Danalache, M. *et al.* Injection of Porcine Adipose Tissue-Derived Stromal Cells by a Novel Waterjet Technology. *Int J Mol Sci.* **22** (8), 3958, doi:10.3390/ijms22083958, (2021).
- 10 Jäger, L. *et al.* A novel waterjet technology for transurethral cystoscopic injection of viable cells in the urethral sphincter complex. *Neurourol Urodyn.* **39** (2), 594-602, doi:10.1002/nau.24261, (2020).
- 11 Linzenbold, W. *et al.* Rapid and precise delivery of cells in the urethral sphincter complex by a novel needle-free waterjet technology. *BJU Int.* **127** (4), 463-472, doi:10.1111/bju.15249, (2021).